N93-13400

ONE-DIMENSIONAL TRANSIENT FINITE DIFFERENCE MODEL OF AN OPERATIONAL SALINITY GRADIENT SOLAR POND

Michael C. Hicks
National Aeronautics and Space Administration
Lewis Research Center
Cleveland, Ohio 44135

Peter Golding
University of Texas at El Paso
El Paso, Texas 79968

SUMMARY

This paper describes the modeling approach used to simulate the transient behavior of a salinity gradient solar pond. A system of finite difference equations are used to generate the time dependent temperature and salinity profiles within the pond. The stability of the pond, as determined by the capacity of the resulting salinity profile to suppress thermal convection within the primary gradient region of the pond, is continually monitored and when necessary adjustments are made to the thickness of the gradient zone. Results of the model are then compared to measurements taken during two representative seasonal periods at the University of Texas at El Paso's (UTEP's) research solar pond.

INTRODUCTION

In a non-convecting salinity gradient solar pond, natural convection is artificially suppressed by establishing an internal region characterized by a strong salinity gradient. The natural buoyancy of the warmer water in the lower regions of the pond is offset by the water's higher density resulting from the higher salt concentration at the corresponding depth. As temperature of the water in the solar pond increases with depth, salt concentration also increases to the extent necessary to ensure that the density of the fluid is continuously increasing.

The stability of the solar pond is a function of the thermal and solutal diffusion rates which in turn have a strong dependence on the localized temperature of the fluid. Internal and boundary stability criteria have been developed that generally determine the necessary localized salinity gradient required to maintain a stable regime for a given temperature profile. These stability relationships have been used in conjunction with a numerical model of the transient temperature and salinity profiles to simulate the eventual erosion of the gradient zone, absent any maintenance intervention. The numerical model described in this work can be used as a predictive tool for determining the approximate shapes of the temperature and salinity profiles which can be expected over an operating period when estimated average daily ambient temperatures and insolation values are provided.

Background

Solar energy incident upon the surface of a shallow pond will be partially transmitted to the bottom of the pond where much of it is absorbed. This normally leads to natural convection as absorbed energy in the lower regions of the pond causes the fluid to thermally expand. Consequently, the thermal energy will be transported to the surface and released. In a non-convecting salinity gradient solar pond this convective process is suppressed by establishing an internal region with a salinity gradient of sufficient strength to ensure that the localized decreases in density due to thermal expansion are counter-balanced by the localized increases in density due to the higher salt concentrations. Thermal conduction will then become the dominant heat transfer release mechanism through the region of the pond where convection is suppressed. Due to the relatively low value of thermal conductivity for water (approximately 0.65 W/m-°C) an "insulating" layer develops which allows temperatures approaching 100 °C in the pond's thermal storage zone.

The typical solar pond is characterized by three regions (Figure 1); a convective surface region referred to as the Upper Convecting Zone (UCZ), a non-convective primary gradient region referred to as the Non-Convecting Zone (NCZ), and a convective thermal storage region referred to as the Lower Convecting Zone (LCZ). The thickness of each of these zones depends upon the season of the year and the manner in which the pond is being operated. For purposes of this analysis average values were derived from the research pond currently in operation at the University of Texas at El Paso (UTEP). The dimensions of this pond are 52.4 m across by 64.0 m long comprising a total surface area of 3,355 m^2 (about 5/6 of an acre). The walls of the solar pond slope inward at an approximate angle of 30° from horizontal. The depth of the pond is about 3.5 meters resulting in an approximate floor area of 2,500 m^2.

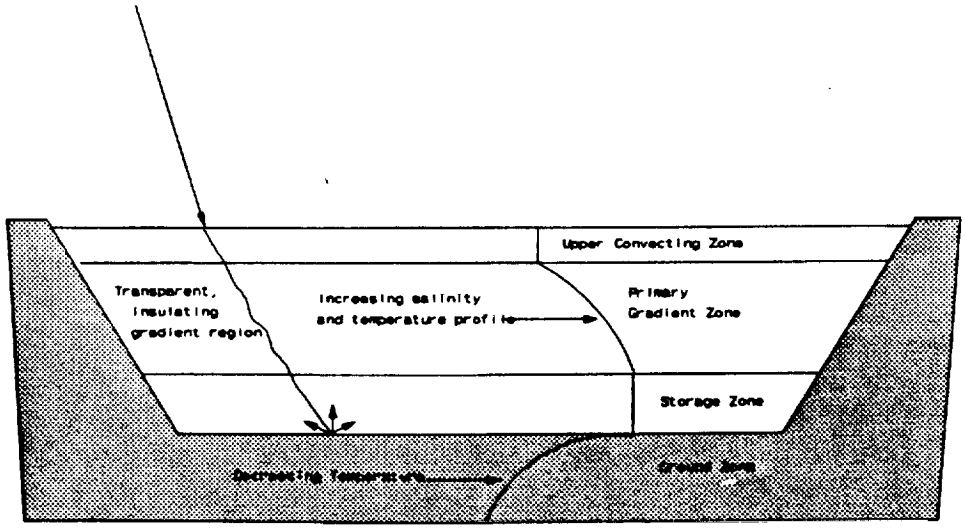

Figure 1. Schematic of a solar pond.

MODELING APPROACH

In developing a solar pond performance model a number of simplifying assumptions can be made to allow for computational ease and modeling efficiency without sacrificing the accuracy of results. This is particularly true if the modeling objective is to simulate macroscopic changes such as gradual drifts in average storage zone temperatures or changes in temperature and salinity profiles over a relatively large period of time.

Derivation of Boundary Conditions

Earlier work was performed by Hull showing that modeling for hourly variations does little to change the results obtained for the LCZ temperature over an extended period of study [1]. Since diurnal fluctuations in ambient temperature and solar insolation have a negligible impact on the solar pond's overall performance, average values of daily insolation and ambient temperature were used for the transient boundary conditions.

An interpolating function was derived for insolation on a horizontal surface from monthly averages obtained over a 21 year period for El Paso, Texas [2]. This is given as follows:

$$I_n = 6{,}300 + 2{,}300 \cdot \sin\left[\frac{2\pi(n-70)}{365.25}\right] \qquad (W/m^2) \qquad \text{Eq. (1)}$$

where: n = day of the year.

The portion of solar radiation incident on a horizontal surface that is reflected at the surface of the air-water interface of the pond is modeled by assuming that the incident radiation is direct beam radiation and intersects the surface at a fixed angle of incidence. These assumptions were previously reviewed by Hull in a comparison of results from a detailed computer model with an analytical model employing the assumption of direct beam radiation. The results showed that accurate estimates of the LCZ temperature can be obtained when the fixed angle of incidence (i.e., A_i) is calculated at solar noon 17 days before the autumnal equinox [1].

The following equation is used to calculate the fixed angle of incidence used in this analysis [2]:

$$\alpha_i = \cos^{-1}(\sin\beta \cdot \sin\gamma + \cos\beta \cdot \cos\gamma \cdot \cos\omega) \qquad \text{Eq. (2)}$$

where:
- γ = latitude of El Paso, Texas (i.e., 31.5°).
- β = declination of sun on the 17th day preceding the autumnal equinox.
- ω = hour angle at solar noon (i.e., 0°).

The angle of declination (β) is the angle of the earth's axis relative to the sun-earth line and is calculated for the 17th day preceding the autumnal equinox as follows:

$$\beta = 23.44° \cdot \sin\frac{(360 \cdot (\delta - 81))}{365.25} \qquad \text{Eq. (3)}$$

where: δ = the day of the year for September 6th (i.e., 249)

This gives a calculated value for α_i of 25.66° which is the fixed angle of incidence used in this analysis. The associated fixed angle of refraction is calculated using Snell's Law by the following relationship:

$$\rho_F = \sin^{-1}\frac{(\sin(\alpha_i))}{n} \qquad \text{Eq. (4)}$$

Using 1.333 for the index of refraction, (n), for the pond's salt water solution [3] Snell's Law yields a value of 18.99° for the fixed angle of refraction, ρ_F.

The surface reflectivity is then calculated using the following relationship derived from Fresnel's equations:

$$\rho_R = .5 \cdot \frac{\sin^2(\alpha_i-\rho_F)}{\sin^2(\alpha_i+\rho_F)} + .5 \cdot \frac{\tan^2(\alpha_i-\rho_F)}{\tan^2(\alpha_i+\rho_F)} \qquad \text{Eq. (5)}$$

Applying the calculated values for the fixed angle of incidence and refraction to this equation yields an effective surface reflectivity (ρ_R) of .021.

The ambient temperature is calculated in a manner similar to that used in developing the average daily insolation. Average daily ambient temperatures are obtained from a periodic interpolating function fitted to actual historical temperatures recorded over a thirty year period by the National Oceanic and Atmospheric Administration.

$$T_a(n) = 63.55 + 19.15 \cdot \sin\frac{(2\pi(n-105))}{365.25} \qquad (°C) \qquad \text{Eq. (6)}$$

where: n = the day of the year.

Pond Attenuation of Solar Radiation

As the radiation is transmitted through the pond it is attenuated along it's path by scattering and absorption. The shorter wavelengths of the solar radiation will be transmitted through the pond with very little absorption, whereas the longer wavelengths (i.e., the infrared portion of the spectrum) will be absorbed within the first few centimeters. Wavelengths longer than the infrared wavelength (i.e., greater than 10^{-6}m) are reflected at the pond's surface.

The absorption and scattering of the solar radiation is generally represented by a transmission function from which the radiation intensity at a given depth can be determined. One such function, developed by Hull, was derived from an extensive set of experimental absorption data measured for pure water. This data was reduced into a four part summation of exponential terms.

$$\tau = \sum_{j=1}^{4} (B_j) \cdot e^{-\alpha_j x} \qquad \text{Eq. (7)}$$

where: τ = the fraction of solar radiation reaching a depth (x).

This reduced function correlates well with a more extensive forty part function, derived from the same data, never deviating by more than .01 in transmittance over a 2 meter interval. The parametric values used for this transmission function are provided in Table I.

Table I Hull Four-Part Transmission Function

Exponential Extinction Coefficients for Water

(j)	B_j	n_j (m^{-1})
1	0.237	0.032
2	0.193	0.450
3	0.167	3.000
4	0.179	35.000

When compared with measurements taken at the UTEP research solar pond on April 20, 1989 the Hull Four-Part function resulted in substantially higher transmittance values, which is to be expected since that transmission function was derived from absorption measurements in pure water. A transmission function was derived from the aforementioned measurements taken at UTEP's research pond. The following third degree polynomial provides an accurate fit to the measured data for distances ranging from 0.0 to 2.6 meters. A plot of this curve fit along with the Hull Four-Part transmission function and a third transmission function developed by Rabl-Nielson [4] have been presented in Figure 2 for comparison.

$$\tau(x) = -.066x^3 + .385x^2 - .768x + .745 \qquad \text{Eq. (8)}$$

Pond Stability Criteria Considerations

The NCZ has been subdivided into two sub-regions to recognize the more stringent stability criterion that exists at the upper and lower interfaces. The internal regions of the NCZ must meet the following dynamic stability criterion [5], at a minimum, in order to ensure that thermal convection in this region is suppressed:

$$G_T < \frac{(Pr+\tau)}{(Pr+1)} \cdot \frac{\beta}{\alpha} \cdot G_s \qquad \text{Eq. (9)}$$

where:
- G_T = the temperature gradient at various locations in the NCZ (°C/m),
- G_s = the salinity gradient at corresponding locations (%/m),
- β = the saline expansion coefficient for NaCl (m^3/Kg),
- α = the thermal expansion coefficient (1/°C),
- Pr = Prandtl number (i.e., ratio of the kinematic viscosity to the thermal diffusivity),
- τ = ratio of the saline diffusivity to the thermal diffusivity (i.e., K_s/K_T).

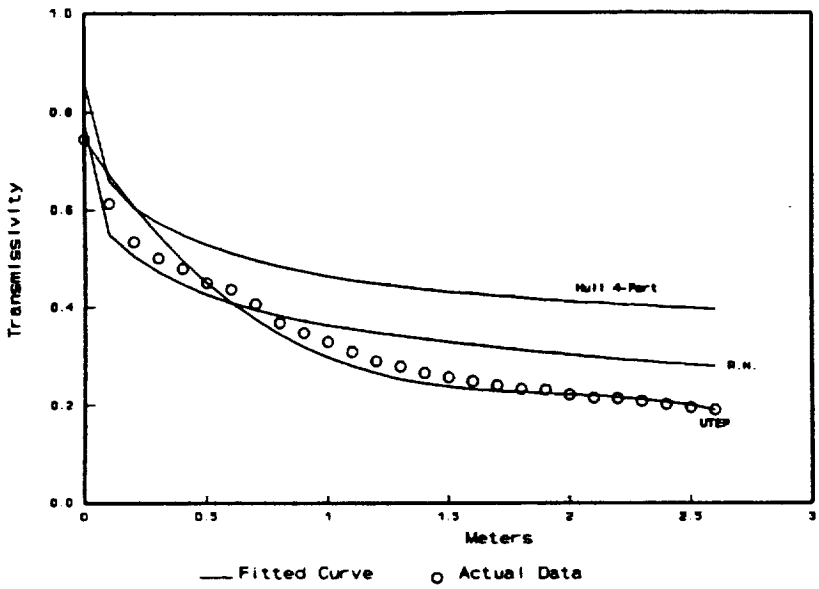

Figure 2. Comparative plot of transmission functions.

Since the values for the parameters in the above equation are dependent on both temperature and salinity it is necessary to develop a functional relationship between the salinity gradient factor (i.e., SGF, and defined as $SGF=[(Pr+\tau)/(Pr+1)]\cdot(\beta/\alpha)$) and temperature [6]. Using information published by the Department of Interior's Office of Saline Water the following relationship was derived [7]:

$$SGF(T) = \frac{(-T^3+198.75^2)}{7{,}812.5} - (1.702)T+48.876 \qquad \text{Eq. (10)}$$

A plot of Equation 10 with the actual data for the SGF is presented in Figure 3. This relationship was then inserted into Equation 9 to obtain the necessary temperature and salinity gradient relationship that was used in establishing the internal threshold salinity gradient.

The dynamic stability criterion that is employed at both the upper and lower NCZ interfaces is based on an empirical relationship derived from Neilsen and is referred to as the Neilsen boundary condition [8]. This empirical relationship is given as follows:

$$G_s = A \cdot G_T^{.63} \qquad \text{Eq. (11)}$$

where: A is set at 28.0 $(Kg/m^4)\cdot(m/K)^{.63}$

Development of Temperature Profile Equations

The nodal equations assume the thermal exchanges that take place between the various zones within the solar pond can be adequately represented by a transient one-dimensional model. Thermal properties of the pond are assumed to be uniform within each of the pond's zones. Using these assumptions, temperature changes, resulting from thermal exchanges within the pond, can then be represented by a

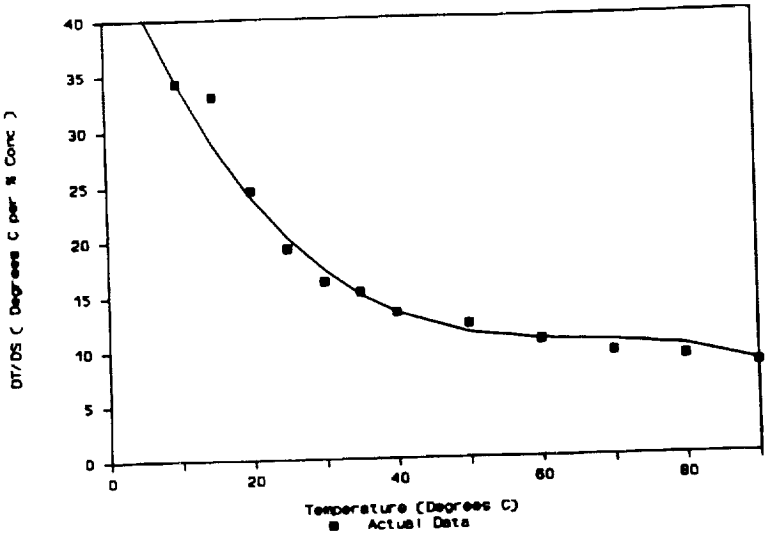

Figure 3. Comparative plot of the SGF interpolating function with actual data.

system of algebraic equations which explicitly solve for the temperature at node (i) and time (j+1) in terms of nodes (i-1, i, i+1) at time (j). These equations are derived by representing Fourier's heat conduction equation by a system of one-dimensional forward-difference equations (where x is positive in the downward direction from the surface at x = 0.0).

Since the UCZ is essentially uniform in temperature it is represented by a single node. It's average daily temperature is set equal to the ambient air temperature (T_a) which establishes the boundary condition for the initial node. The LCZ is similarly treated by assuming no temperature gradient throughout the zone. Solar radiation reaching the depth of the NCZ-LCZ interface, and beyond, is assumed to be completely absorbed within the LCZ. A ground zone (GRZ) is modeled, in the same fashion as the NCZ, by a representative nodal network that continues to a depth where it can be reasonably assumed that a constant ambient temperature exists.

UCZ-Nodal Equation:

$$T_{UCZ} = T_a(t) \qquad \text{Eq. (12)}$$

UCZ-NCZ Interface Nodal Equation:

$$T_{0,j+1} = T_{0,j}(1-2Fo-2Fo \cdot Bi)+2Fo \cdot (T_{i,j}+Bi \cdot T_{UCZ,j})+\frac{2Bi \cdot Fo}{h_c} \cdot (I_{i-1/2,j}-I_{i+1/2,j}) \qquad \text{Eq. (13)}$$

NCZ Interior Nodal Equations:

$$T_{i,j+1} = T_{i,j} \cdot (1-2Fo) + Fo \cdot (T_{i+1,j}+T_{i-1,j}) + \frac{\delta x_n \cdot Fo}{K_n} \cdot (I_{i-1/2,j}-I_{i+1/2,j}) \qquad \text{Eq. (14)}$$

NCZ-LCZ Interface Nodal Equation:

$$T_{n,j+1} = T_{n,j} \cdot (1 - 2Fo - 2Fo \cdot Bi) + 2Fo \cdot (T_{n-1,j} + Bi \cdot T_{LCZ,j}) + \frac{2Bi \cdot Fo}{h_c} \cdot (I_{n-1/2,j} - I_{n+1/2,j}) \quad \text{Eq. (15)}$$

LCZ Interior Nodal Equation:

$$T_{LCZ,j+1} = T_{LCZ,j} \cdot (1 - 2H) + H \cdot (T_{n,j} + T_{0,j}) + \frac{H}{h_c} \cdot (I_{NCZ/LCZ} + q_j) \quad \text{Eq. (16)}$$

$$\textit{where:} \quad H = \frac{dt \cdot h_c}{L_{LCZ} \cdot \rho \cdot C_p}$$

LCZ-GRZ Interfacial Nodal Equation:

$$T_{0,j+1} = T_{0,j} \cdot (1 - 2Fo - 2Fo \cdot Bi) + 2Fo \cdot (T_{1,j} + Bi \cdot T_{LCZ,j}) \quad \text{Eq. (17)}$$

GRZ Interior Nodal Equation:

$$T_{k,j+1} = T_{k,j} \cdot (1 - 2Fo) + Fo \cdot (T_{k+1,j} + T_{k-1,j}) \quad \text{Eq. (18)}$$

In the above equations $T_{UCZ,j}$ and $T_{LCZ,j}$ are the bulk temperatures of the UCZ and LCZ at time (j), respectively, Fo is the Fourier Modulus, and Bi is the Biot modulus. The heat transfer coefficient is set at 263 W/m^2-°C and is assumed to be the same at both interfaces. This value is derived from consideration of the empirical relationship developed for two horizontal plates.

Development of Salinity Profile Equations

The salinity profile is derived from the solution of a transient one dimensional partial differential equation wherein the rate of salinity change is presented as a function of the temperature dependent solutal diffusivity (K_s) and the rate of change of salinity with respect to depth in the gradient zone. After the salinity profile is calculated for each progression in temperature profile it is checked to ensure that the stability criteria at both the upper and lower boundaries as well as within the NCZ are satisfied. If the boundary stability criterion at either the upper or lower interfaces is not met the boundary is repositioned until the stability criterion is satisfied. If the internal stability criterion is not met the run is simply terminated with the creation of a file containing the last temperature and salinity profiles. Changes to the salinity profile are based upon a numerical solution of the following differential equation describing the time dependent behavior of the salinity profile in the absence of any fresh water or brine injection into the UCZ.

$$\frac{\partial S}{\partial t} = \frac{1}{R(z)} \cdot \frac{\partial}{\partial z} \left\{ R(z) \cdot K_s \cdot \left[\frac{\partial s}{\partial z} + S_T \cdot S(1 - \frac{S}{\rho}) \cdot \frac{\partial T}{\partial z} \right] \right\} \quad \text{Eq. (19)}$$

where: R(z) = the ratio of surface area at depth (z) to the surface area at the top

of the NCZ. This term only has significance in small ponds with sloping side walls.

K_s = the temperature dependent solutal diffusivity of NaCl which represents the rate of molecular diffusion of NaCl in the presence of a salinity gradient.

S_T = is the Soret coefficient reflecting the secondary salt transport process that occurs in the presence of a temperature gradient.

The above equation has been simplified by considering that the Soret coefficient for NaCl solutions is of the order of $1x10^{-3}$ 1/K to $3x10^{-3}$ 1/K and that for most salinity gradients it's contribution to salt transport will be relatively small. This was evidenced in analyses performed at Ohio State University, where the observed salt transport differed from the calculated salt transport, using Equation 19 without the S_T term, by less than 10% [8].

The second simplifying adjustment made to Equation 19 reflects the relative constancy of the solutal diffusivity coefficient, K_s, with variations in salinity concentrations. Generally, K_s is dependent upon both the temperature and salinity of the solution. However, for NaCl solutions the variance of K_s with salinity, over the salinity range of 0% to 30% by weight is negligible for purposes of this work. The dependence of Ks on temperature, however, results in an increase on the order of 400% over temperatures ranging from 5°C to 90°C. Therefore, a functional relationship was derived in the form of a second degree polynomial from data obtained from the Department of Interior's Office of Saline Water [7].

$$K_s(T) = (T^2 + 95.56T + 2920.9) \cdot 9.23 \times 10^{-10} \qquad (m^2/hr) \qquad \text{Eq. (20)}$$

Finally, the term containing information on the physical aspects of the pond walls (i.e., R(z)) is only important for small area ponds. Generally, the presence of sloping walls in a solar pond decreases the salinity gradient at the upper levels of the NCZ. It has been found [8] that for solar ponds with an area of 10,000 m^2 and a geometric factor of approximately .05 (defined as the ratio of NCZ thickness to pond length multiplied by twice the cotangent of the wall's angle with horizontal) that the maximum difference between an analysis with and without the effects of the wall slope on the salinity gradient taken into consideration is 5%. The geometric factor for UTEP's solar pond is approximately .09 (assuming a characteristic pond length of 64 m, a NCZ thickness of 1.5 m, and an angle of 300 from horizontal) which gives, from interpolation of plotted data, a maximum difference in salinity gradient of approximately 10%. The error introduced by excluding this effect is partially offset by the fact that the Soret coefficient is not included in this analysis. In light of the above considerations the diffusion rate equation can be reduced to the following;

$$\frac{\partial S}{\partial t} = K_s \cdot \frac{\partial^2 S}{\partial z^2} \qquad \left[\frac{kg}{m^3\text{-}day}\right] \qquad \text{Eq. (21)}$$

where: K_s is expressed in the solution as a temperature dependent parameter whose functional relationship is given by Equation 20.

This equation was numerically approximated in a manner similar to that used in developing the solution for the temperature profile. A nodal network, with internodal distances corresponding to that used in the determination of the temperature profile, was constructed with nodes placed at the upper and lower

interfaces of the GRZ. The forward difference equations for the salinity profile nodes are given as follows:

Boundary:

$$S_{n,j+1} = S_{n,j} \cdot \left[\frac{\Delta t}{\Delta X_n^2}\right] \cdot \left[\frac{\Delta X_n^2}{\Delta t} - 2K_{s_1} - K_{s_2}\right] + \left[\frac{\Delta t}{\Delta X_n^2}\right] \cdot \left[2(S_{n,j} \cdot K_{s_n} + (S_{n-1,j}) \cdot K_{s_2}\right] \quad \text{Eq. (22)}$$

Internal:

$$S_{n,j+1} = S_{n,j} \cdot \left[\frac{\Delta t}{\Delta X_n^2}\right] \cdot \left[\frac{\Delta X_n^2}{\Delta t} - K_{s_1} - K_{s_2}\right] + \frac{\Delta t}{\Delta X_n^2} \cdot \left[S_{n+1,j} \cdot K_{s_1} + S_{n-1,j} \cdot K_{s_2}\right] \quad \text{Eq. (23)}$$

UCZ Node:

$$S_{1,j+1} = S_{1,j} + (S_{2,j} - S_{1,j}) \cdot 2(K_{s_1}) \cdot \frac{\Delta t}{\Delta X_n \cdot L_{UCZ}} \quad \text{Eq. (24)}$$

where:

S	=	the salinity expressed in terms of concentration (i.e., kg/m^3)
K_{sn}	=	the solutal diffusivity expressed in m^2/Day at the interface temperature.
K_{s1}	=	the solutal diffusivity at the upper node's temperature (m^2/Day).
K_{s2}	=	the solutal diffusivity at the lower node's temperature (m^2/Day).
L_{UCZ}	=	the upperzone thickness.

Discussion of Results

Two validation runs were performed to assess the accuracy of the computed temperature profile over a span of time. A summer month (i.e., August, 1989) and a winter month (i.e., November, 1989) were selected and actual measurements, to the extent available, were collected.

August 1989 Validation Run: Actual measurements taken at the UTEP research pond were used for the daily ambient temperature, heat extraction from the storage zone, daily solar insolation, and weekly pond profiles for temperature and salinity. The run period extended from August 2, 1989 through August 31, 1989 for a total of 30 days. A plot of the calculated temperature profile on the last day is plotted against actual temperature readings taken on that same day. As can be seen from the comparative plot, Figure 4, a close correlation of computed temperature with actual temperature exists throughout the NCZ. Only a slight variance between computed and actual storage zone temperatures exists (about .97°C or 1.3% from actual).

November 1989 Validation Run: In this run an initial temperature profile was constructed from pond measurements taken on November 7, 1989. During the run period, which spanned 22 days (from 11/7/89 through 11/28/89), the salinity gradient was not sufficiently steep at the upper and lower boundaries and an adjustment to the thickness of the primary gradient region was necessary.

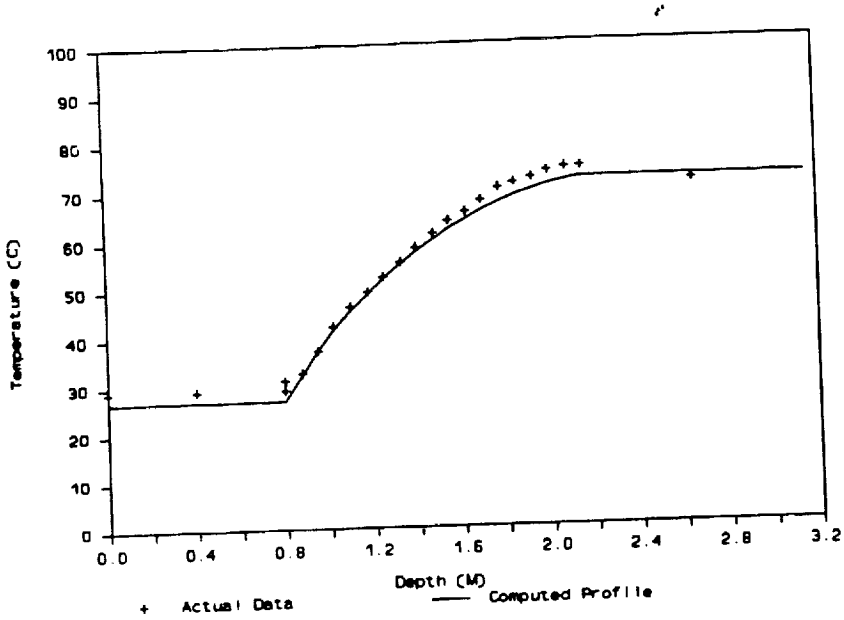

Figure 4. Comparative plot of temperature profiles for 8/31/89.

A comparative plot of the computed temperature profile on the 28th day along with actual measurements is provided in Figure 5. As with the previous August run, the results correlate well with measurements taken at the pond. The temperature variance at the mid point in the storage zone is 5.0°C (i.e., approximately 10.0% of actual). This higher variance is primarily due to the fact that the LCZ exhibited a pronounced temperature stratification (which was not modeled) during this period of time. The resulting salinity profile, derived from this temperature profile, is presented in Figure 6. As previously mentioned, a boundary adjustment occurred at both the upper and lower NCZ interfaces in order to satisfy the boundary stability criterion.

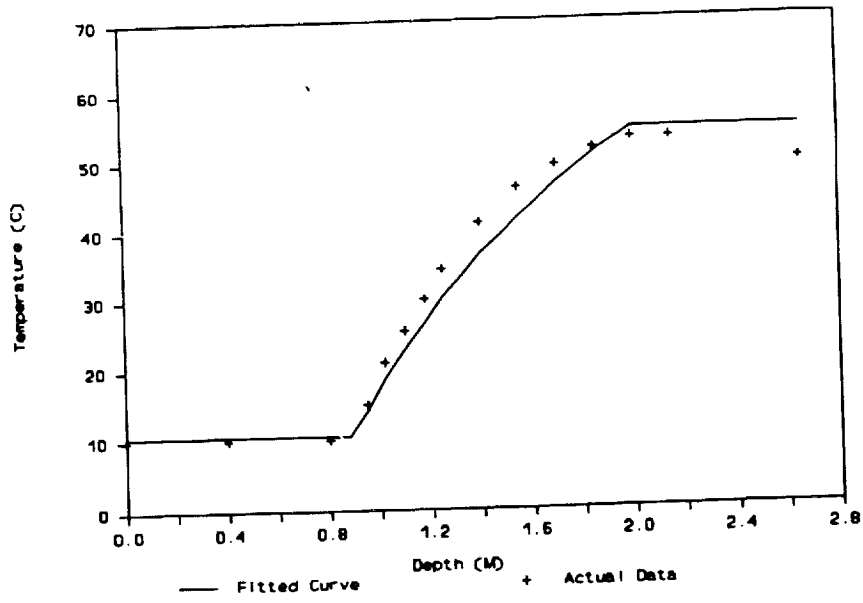

Figure 5. Comparative plot of temperature profiles for 11/28/89.

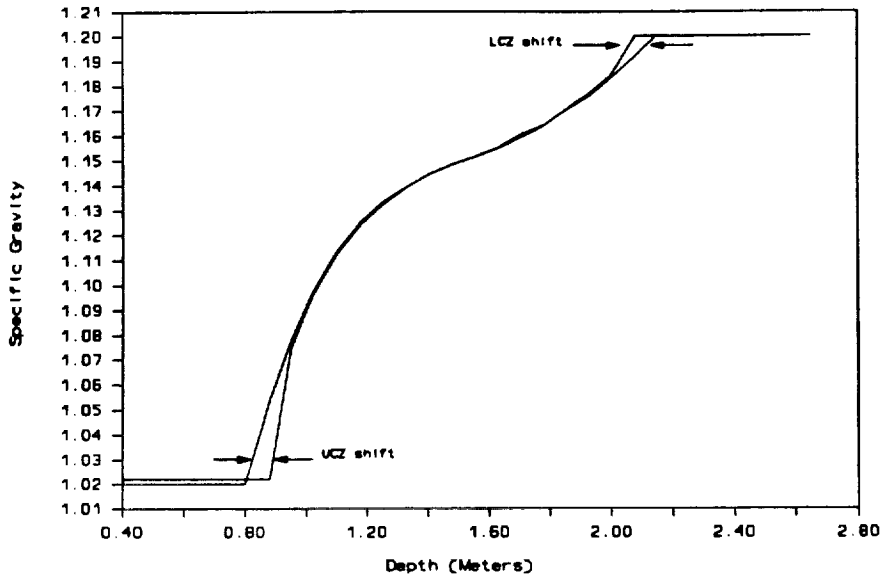

Figure 6. Transition in salinity profile resulting from shifts in NCZ boundaries.

CONCLUSIONS

The double diffusive transfer processes typical of a salinity gradient solar pond was represented by a system of coupled finite difference equations to simulate the interdependency of the ponds temperature and salinity gradients. A number of simplifying assumptions can be readily made to allow for an easily generated solar pond numerical model that will provide a reasonable first order prediction of changes in temperature and salinity profiles, bulk temperature changes in the ponds storage zone, and changes in the thickness of the gradient zone. This modeling approach may be used for predicting attainable storage temperatures, gradient zone maintenance schedules, and salinity concentration requirements. It is applicable to a variety of conditions for purposes of determining the economic viability of a new solar pond and could be employed in the operational planning of currently operating solar ponds. The results also provide valuable insight into the salinity profiles which need to be installed in order to maintain a stable thermal stratification in an established solar pond (for a given storage zone temperature associated with a given application). Further, the time variance calculation of the profiles provides useful predictions of the salinity gradient modifications which need to be accomplished during the time evolution of the operating pond in order to sustain operation.

REFERENCES

1. Hull, J. R. : Computer Simulation of Solar Pond Thermal Behavior. Solar Energy, vol. 25, 1980, pp. 33-40.

2. Richards, L. M. and Bush, G. E. : Solar Geometry and Time. Solar Energy Technology

Handbook, 1980, pp. 39-65.

3. Weinberger, H. : The Physics of the Solar Pond. Solar Energy, vol. 8, 1963, pp. 45-56.

4. Knudsen, J. D. : Numerical Simulation of Large Scale Solar Ponds. Master Thesis for University of Texas at El Paso, 1987.

5. Elwell, D. L., Short, T. H., and Badger, P. C. : Stability Criteria for Solar (Thermal-Saline) Ponds. Journal Series No. 68-77, Ohio Agricultural Research and Development Center.

6. Hicks, M. C. : Computer Performance Model of a Solar Pond-Coupled Desalination System. Master Thesis for University of Texas at El Paso, 1990.

7. Saline Water Conversion Engineering Data Book. Office of Saline Water, 2nd Ed., United States Department of the Interior, 1971.

8. Hull, J. R., Nielsen, C. E., and Golding, P. : Salinity-Gradient Solar Ponds. CRC Press.

9. Akbarzadeh, A. : Effect of Sloping Walls on Salt Concentration Profile in a Solar Pond. Solar Energy, vol. 33, 1984, pp. 137-141.